Mol Biol Rep (2011) 38:3765–3776
DOI 10.1007/s11033-010-0492-5

Cloning, expression and dynamic simulation of TRYP6 from *Leishmania major* (MRHO/IR/75/ER)

G. Eslami · F. Frikha · R. Salehi · A. Khamesipour · H. Hejazi · M. A. Nilforoushzadeh

Received: 13 December 2009 / Accepted: 10 November 2010 / Published online: 1 December 2010

Abstract *Leishmania,* a digenetic protozoan parasite causes severe diseases in human and animals. Efficient evasion of toxic microbicidal molecules, such as reactive oxygen species and reactive nitrogen species is crucial for *Leishmania* to survive and replicate in the host cells. Tryparedoxin peroxidase, a member of peroxiredoxins family, is vital for parasite survival in the presence of antioxidant, hence it is one of the most important molecules in *Leishmania* viability and then, it may be an appropriate goal for challenging against leishmaniasis. After cloning and sub-cloning of TRYP6 from *Leishmania major* (MRHO/IR/75/ER), homology modeling of the *Lm*TRYP6 was proposed to predict some functional property of this protein. The refined model showed that the core structure consists of a seven β stranded β-sheet and five α helices which are organized as a central 7-stranded β2-β1-β5-β4-β3-β6-β7 surrounded by 2-stranded β-hairpin, α helices A and D on one side, and α helices B, C and E on the other side. The peroxidatic active site is located in a pocket formed by the residue Pro45, Met46, Thr49, Val51, Cys52, Arg128, Met147 and Pro 148. The catalytic Cys52, located in the first turn of helix αB, is in van der Waals with a Pro45, a Thr49 and an Arg128 that are absolutely conserved in all known Prx sequences. In this study, an attractive molecular target was studied. These results might be used in designing of drugs to fight an important human pathogen.

Keywords Tryparedoxin peroxidase · *L. major* · Homology modeling · Molecular dynamics

G. Eslami (✉)
Department of Parasitology and Mycology, Shahid Sadoughi University of Medical Sciences, 8916188/35 Yazd, Iran
e-mail: eslami_g2000@yahoo.com; g_eslami@ssu.ac.ir

F. Frikha
Laboratoire de Biochimie et de Génie Enzymatique des Lipases, École Nationale d'Ingénieurs de Sfax, Route Soukra Km 3.5 B.P W, 1173 Sfax, Tunisia

R. Salehi
Department of Genetics and Molecular Biology, Faculty of Medicine, Isfahan University of Medical Sciences, Isfahan, Iran

A. Khamesipour · M. A. Nilforoushzadeh
Center for Research and Training in Skin Disease and Leprosy, Tehran University of Medical Sciences, 415 Taleghani Avenue, 1416613675 Tehran, Iran

H. Hejazi
Department of Parasitology and Mycology, Faculty of Medicine, Isfahan University of Medical Sciences, Isfahan, Iran

M. A. Nilforoushzadeh
Skin Diseases and Leishmaniasis Research Center, Isfahan University of Medical Sciences, Isfahan, Iran

Introduction

Leishmania, a digenetic protozoan parasite shuttling specifically between a flagellated promastigotes in the gut of the sand fly and an intracellular amastigotes in the mammalian macrophages, causes severe diseases in human and animals. Efficient evasion of toxic microbicidal molecules such as reactive oxygen species (ROS) and reactive nitrogen species (RNS), produced at each stage of infection, is crucial for *Leishmania* to survive and replicate in the host cells [1, 2]. Peroxiredoxin family including tryparedoxin peroxidase (TRYP) of *Leishmania* was shown to be vital for parasite survival in the presence of antioxidant [3–8]. The most famous function for this family is antioxidant

role and subsequently survival of *Leishmania* parasite in the host cells [9–12]. Also, other functions have been attributed to tryparedoxin peroxidase including protection of the mitochondrial genome from direct or indirect peroxide-mediated damage [13]. Its role in arsenite resistant [11] and metastasis [12] are defined which strength the link between parasite virulence and antioxidant defense [12]. Peroxiredoxins are shown to possess peroxinitrite reductase activity and participate in detoxification of ROS [14, 15]. Therefore due to its involvement in vast array of biological phenomenon, tryparedoxin peroxidase aimed as a target for investigation.

In *Leishmania* spp. like *L. amazonensis* [11], *L. infantum* [16, 17], *L. donovani* [18] and *L. major* [8], more than one peroxiredoxins have been described. *L. donovani* and *L. infantum* contain both cytosolic and mitochondrial forms of tryparedoxin peroxidase [11, 13, 17, 18]. Cytosolic tryparedoxin peroxidase would be important for oxidative stress because the first line of oxidative stress products would be in the cytosol. *L. chagasi* has different isogenes which are responsible for the expression of three very similar peroxiredoxins [19]. As shown in genedb (www.genedb.org), the genes encoding tryparedoxin peroxidase in *L. major* comprise TRYP1 (tryparedoxin peroxidase), TRYP2 (tryparedoxin peroxidase, TXNPx, PXN1, TSA), TRYP3 (tryparedoxin peroxidase, TXNPx, PXN3, TSA), TRYP4 (tryparedoxin peroxidase, TSA, TXNPx, PXN), TRYP5 (tryparedoxin peroxidase, TXNPx, PXN, TSA), TRYP6 (tryparedoxin peroxidase, TXNPx, PXN, TSA), and TRYP7 (tryparedoxin peroxidase) that present on chromosome 15 in a tandem array. TRYPs 1, 3, 5 and 7 encode a predicted protein with 199 amino acids whereas TRYPs 2, 4 and 6 code for a predicted protein with 191 amino acids [8]. To our knowledge there is no report on *TRYP6* gene sequence from *L. major* (MRHO/IR/75/ER), as an approved Iranian isolate which is used for leishmanization and preparation of Old World experimental *Leishmania* vaccine and leishmanin [20–25].

In this study, full-length gene sequence and its encoded protein of the *lmTRYP6* gene is reported, the gene sequence was also compared with *LmTRYP6* (LmjF15.1140), another previously reported member of this gene family. Homology modeling was proposed to predict some functional properties of its virtual protein.

Materials and methods

Parasites

Leishmania major promastigotes (MRHO/IR/75/ER) were grown at 26 ± 1°C in RPMI 1640 medium (Sigma, USA) supplemented with 10% fetal calf serum (FCS, Sigma), 100 U/ml penicillin G and 100 μg/ml streptomycin [26–28].

DNA extraction

DNA extraction was done based on method described by Eisenberger and Jaffe [29] with a minor modification. SDS (10%) was used instead of Triton X-100 (1%). The extracted DNA sample was quantified and analyzed by agarose gel electrophoresis.

RNA extraction

RNA extraction was performed using RNX^{TM} solution (CinnaGen) according to the manufacturer instruction. The sample was quantified and analyzed by agarose gel electrophoresis under RNAse free condition.

cDNA synthesis

Using RevertAid^{TM} First Strand cDNA Synthesis Kit (#K1621, Fermentas), cDNA was synthesized according to the manufacturer instruction.

Primers

Sense and antisense oligonucleotide primers were designed based on the nucleotide sequence data of *LmTRYP6* gene (LmjF15. 1140) obtained from Genbank. The sequences of sense and antisense primers used in this study are: 5′-ATG TCCTGCGGTAA-CGCCAAG-3′ and 5′-TTACTTGTTG TGG-TCGACCTTCATGC-3′.

PCR, RT-PCR and sequence analysis

PCR amplification was performed using *L. major* genomic DNA or cDNA as template. PCR master mix contained 10 mM Tris–HCl pH 8.3, 50 mM KCl, 1.5 mM MgCl2, 0.2 mM each dNTPs, 20 pmol of each primer and 0.5 unit of Taq polymerase (Fermentas). Thermal cycling was applied as follow: 94°C for 5 min as initial denaturation, 30 cycles with 94°C for 45 s, 63°C for 45 s and 72°C for 45 s. The final 1 cycle of 72°C applied for 20 min. The PCR product was analyzed by agarose gel and the bands contained amplified products were purified using High Pure PCR Product Purification Kit (#11732668001, Roche).

Cloning of *LmTRYP6* in pTZ57R/T

This step was performed using InsT/Aclone^{TM} PCR Product Cloning Kit (Fermentas) according to the manufacturer instruction. The recombinant plasmid was transformed into *E. coli* XL1-Blue. To confirm the ligation

reaction success, restriction digest was performed on isolated plasmids and the size of the linearized recombinant vector was assessed by agarose gel electrophoresis.

Cloning of *LmTRYP6* in pET15b

The insert of pTZ57R/T was isolated using restriction enzyme digestion and ligated into pET15b expression vector using T4 DNA ligase. The recombinant DNA was transformed into *E. coli* BL21. The in-frame cloning was verified by sequence analysis of the isolated insert from purified vector. After this verification step, in vitro protein expression of *Lm*TRYP6 was carried out.

Expression of *Lm*TRYP6 protein in vitro

The cultured bacteria harboring recombinant plasmids were induced to express by adding IPTG (final concentration 1 mM) into the culture medium. The protein was purified after 2, 4, 6 and 24 h post induction and analyzed by SDS-PAGE and Western blot.

Characterization and molecular analysis

Except for some peroxiredoxin genes in some species, structural data on individual *Lm*TRYP6 is limited; therefore theoretical homology modeling in combination with molecular dynamics (MD) simulations remains an important tool for structure–function analysis of the protein. Characterization of the *Lm*TRYP6 protein from this novel gene was carried out using Basic Local Alignment Search Tool (BLAST) analysis, secondary structure prediction and infrastructural analysis.

The whole sequence of *LmTRYP6* was used to build up 3D structures by means of Molecular Operating Environment 2008.10 program. The *LmTRYP6* sequence was used as a query to search the PDB for homologous sequences of known structures using BLAST P [30, 31].

Protein database searching and sequence analyzing

BLAST P was used to identify the sequence similarities with several members of peroxiredoxin family for selecting the 3D models of the closest homologs available in the Protein Data Bank (PDB) with the least *E* value [30, 31].

Computational methods for building 3D structure

The structure of mentioned template was obtained from the PDB (http://www.rcsb.org/pdb). This structure offered the possibility of exploring the molecular infrastructure via structure-based models and simulations. The 3D model of *Lm*TRYP6 was built by homology modeling using the resolved structure of *Cf*TryP (PDB code 1e2y) as template with 92% amino acids sequence of identity. The Molecular Operating Environment 2008.10 (MOE) software was used for homology modeling, molecular dynamics and structures visualization. The models were stereochemically evaluated using the program PROCHECK. The figures were generated by PyMol program (http://www.pymol.org). The model was subjected to molecular mechanics optimization using CHARMM27 force field, until the gradient of 0.01 kcal/(Å mol) was reached.

Molecular dynamics simulations

Molecular dynamic simulations were carried out at 101 kPa using Nosé-Poincaré-Anderson equations of motion (NPA Algorithm), rigid water and light bonds constrain, relative accuracy of 1e−012, time step of 0.002 ps, temperature response of 0.2 ps and pressure response of 5 ps. The root mean square deviation (RMSD) and the root mean square fluctuation (RMSF) values for the backbone atoms were used to understand the flexibility of the protein.

Results

Gene cloning

The PCR and RT-PCR products showed exactly equal size of *LmTRYP6* gene on agarose gel. After cloning of *LmTRYP6* gene and subsequently confirming by restriction enzyme digestion using *Bam*HI and *Nde*I, The 555 bp fragments were cut from pTZ57R/T vectors and cloned in the dephosphorylated pET15b. The recombinant pET15b plasmids were transferred into *E. coli* BL21 in order to propagating through bacteria. Isolated recombinant DNA plasmids were confirmed by restriction enzyme digestion and sequencing.

In vitro expression of *Lm*TRYP6 protein

IPTG induced recombinant *Lm*TRYP6 protein was expressed in *E. coli* BL21, analyzed and characterized using SDS-PAGE and Western blot methods.

Sequence analyzing and protein database searching

Based on the presented sequence of *LmTRYP6* gene and the one in *L. major, Friedlin* (systemic name LmjF15.1140), the sequence alignment with BioEdit Version 4.8.4 software showed only 79.6% homology between them. *LmTRYP6* showed a deletion in nonconserved sequence toward C-terminal end from nucleotide 531–548 (3.1%

Table 1 BLAST analysis and homology percentage of the Query (*Lm*TRYP6) with the subjects

Subjects	PDB code	Identity (%)
Chains A, B and C of tryparedoxin peroxidase from *Crithidia fasciculate*	1E2YA, B, C	92
Chains A, B and C of tryparedoxin peroxidase from *Trypanosoma cruzi* in the reduced state	1UUL A, B, C	70
Chains A, B of crystal structure from a mammalian 2-Cys peroxiredoxin, Hbp23	1QQ2 A, B	58
Chains A, B crystal structure of human peroxiredoxin I in complex with sulfiredoxin	2RII A, B	58
Chains A, B and C of crystal structure analysis of rat Hbp23PEROXIREDOXIN I from Cys52Ser Mutant	2Z9S A, B, C	57
Chains A, B and C of thioredoxin peroxidase B from Red Blood Cells	1QMV A, B, C	57
Chain A, B and C of crystal structure analysis of bovine mitochondrial peroxiredoxin	1ZYE A, B, C	59

```
                    10        20        30        40        50        60
                ....|....|....|....|....|....|....|....|....|....|....|
CfTryP    1     MSCGAAKLNHPAPEFDDMALMPNGTFKKVSLSSYKGKYVVLFFYPMDFTFVCPTEIIQFS  60
LmTRYP6   1     MSCGNAKLNHPAPEFDVMALMPNGTFKKVSLSSYKGKYVVLFFYPMDFTFVCPTEIIQFS  60

                    70        80        90       100       110       120
                ....|....|....|....|....|....|....|....|....|....|....|
CfTryP    61    DDAKRFAEINTEVISCSCDSEYSHLQWTSVDRKKGGLGPMAIPMLADKTKAIARAYGVLD  120
LmTRYP6   61    DDAKRFAEINTEVISCSCDSEYSHLQWTSVDRKKGGLGPMAIPMLADKTKAIARAYGVLD  120

                   130       140       150       160       170       180
                ....|....|....|....|....|....|....|....|....|....|....|....|
CfTryP    121   EDSGVAYRGVFIIDPNGKLRQIIINDMPIGRNVEEVIRLVEALQFVEEHGEVCPANWKKG  180
LmTRYP6   121   EDSGVAYRGVFIIDPNGKLRQIIINDMPIGRNVEEVIRLVEALQFVEEHGEVCPANCMKV  180


                ....|...
CfTryP    181   DAKKKEGH  188
LmTRYP6   181   DHNK----  184
```

Score = 918.0, Identities = 177/188 (94%), Positives = 177/188 (94%), Gaps = 4/188 (2%)

Score = 918.0, Identities = 177/188 (94%), Positives = 177/188 (94%), Gaps = 4/188 (2%)

```
CfTryP      1 MSCGAAKLNHPAPEFDDMALMPNGTFKKVSLSSYKGKYVVLFFYPMDFTFVCPTEIIQFS  60
              MSCG AKLNHPAPEFD MALMPNGTFKKVSLSSYKGKYVVLFFYPMDFTFVCPTEIIQFS
LmTRYP6     1 MSCGNAKLNHPAPEFDVMALMPNGTFKKVSLSSYKGKYVVLFFYPMDFTFVCPTEIIQFS  60

CfTryP     61 DDAKRFAEINTEVISCSCDSEYSHLQWTSVDRKKGGLGPMAIPMLADKTKAIARAYGVLD 120
              DDAKRFAEINTEVISCSCDSEYSHLQWTSVDRKKGGLGPMAIPMLADKTKAIARAYGVLD
LmTRYP6     61 DDAKRFAEINTEVISCSCDSEYSHLQWTSVDRKKGGLGPMAIPMLADKTKAIARAYGVLD 120

CfTryP    121 EDSGVAYRGVFIIDPNGKLRQIIINDMPIGRNVEEVIRLVEALQFVEEHGEVCPANWKKG 180
              EDSGVAYRGVFIIDPNGKLRQIIINDMPIGRNVEEVIRLVEALQFVEEHGEVCPAN  K
LmTRYP6   121 EDSGVAYRGVFIIDPNGKLRQIIINDMPIGRNVEEVIRLVEALQFVEEHGEVCPANCMKV 180

CfTryP    181 DAKKKEGH 188
                D  K
LmTRYP6   181 DHNK---- 184
```

Fig. 1 Pair wise alignment of *Lm*TRYP6 and *Cf*TryP amino acid sequences

deletion). There is also variations in nucleotide content of *LmTRYP6* compromise 34 A and T nucleotides which replaced by C or G, and 25 C and G nucleotides replaced by A or T. The BLAST search against the deduced amino acid sequence of *LmTRYP6* from *L. major* (MRHO/IR/75/ER) resulted in the identification of 20 sequences from

different species with a high homology (at least to 30%). Sequence analysis showed two highly conserved cysteines (C52 and C173) each embedded in a Valine-Cysteine-Proline (VCP) motif in *LmTRYP6*. BLAST analysis showed that *LmTRYP6* is closely related to *Cf*TryP sequence with the percentage identity of 92% (Table 1).

Homology modeling of *Lm*TRYP6 protein

*Lm*TRYP6 and *Cf*TryP differed from each other by five amino acids including Asn in place of Ala, Val in place of Asp, Cys in place of Trp, Met in place of Lys and Val in place of Gly (Fig. 1). A high level of sequence identity should guarantee more accurate alignment between the target sequence and template structure. The BLAST search resulted in the identification of the crystal structure of *Cf*TryP (PDB code = 1E2Y) from *Crithidia fasciculata* with a high level of sequence identity with *Lm*TRYP6. The identity of this protein with *Lm*TRYP6 was found to be 92%. The single crystal structure of *Cf*Tryp (PDBID = 1e2y) with a resolution of 3.2 Å was selected as the template. The *Cf*TRYP6 crystal structure has been resolved by Alphey et al. (2000).

Validation of *Lm*TRYP6

The RMS deviations between the initial and the optimized models were 0.67 Å (involving α-carbons), 0.69 Å (involving main atoms) and 1.28 Å (involving all atoms). The geometry of the final refined models was evaluated with Ramachandran's plot calculations computed with the PROCHECK program. The Ramachandran plot statistics showed that in *Lm*TRYP6, 89.2% of the residues (141 amino acids) in most favoured regions, 7.6% of the residues (12 amino acids) were found in additional allowed regions, 1.3% of the residues (2 amino acids) were found in generously allowed regions and finally, 1.9% of the residues (3 amino acids) were found in disallowed regions (Fig. 2). The data indicated that the final refined model had appropriate stereochemistry properties for further analysis.

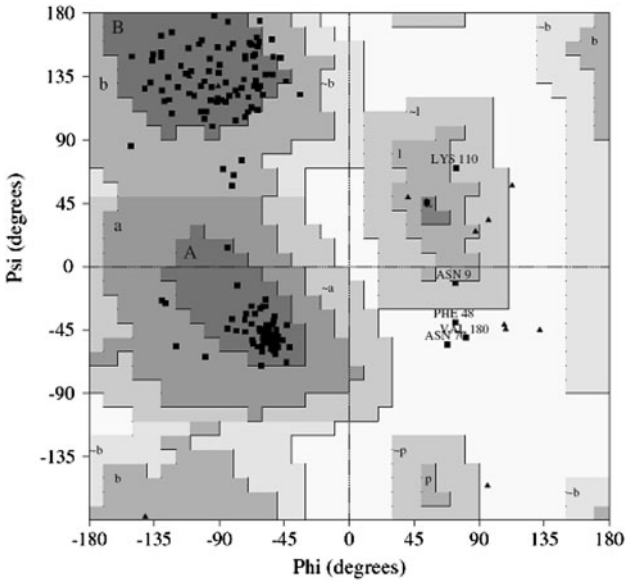

Fig. 2 The Ramachandran's plot calculation of *Lm*TRYP6 was carried out using PROCHECK program

Molecular dynamic simulation

After minimization, the system heating, equilibration and data sampling were carried out in turn for the *Lm*TRYP6 model and for the *Cf*TRYP, respectively. The system heating was performed gradually from 0 to 310 K in a NVT ensemble (constant: N—number of particles, V—volume and T—temperature) and equilibrated for 100 ps, followed until 1 ns simulation for data sampling in a NPT ensemble (constant: N—number of particles, P—pressure and T—temperature).

Prediction of secondary structure of *Lm*TRYP6 protein

The secondary structure prediction (Fig. 3) was carried out using AntheProt 2000V. 5.2 (http://antheprot-pbil.ibcp.fr). The secondary structure of template and final refined model of *Lm*TRYP6 protein appeared to be highly conserved and showed close similarity to the whole structures of template indicating that final structure is reliable. The aligned protein of *Lm*TRYP6 with the template contain α/β hydrolase fold similar to that present in all peroxiredoxins (Fig. 4). The core structure consists of a seven stranded β-sheet and five α helices which are organized as a central 7-stranded β2-β1-β5-β4-β3-β6-β7 (strand β1 and β6 are anti-parallel) surrounded by 2-stranded β-hairpin, α helices A and D on one side, and α helices B, C and E on the other side.

Active site identification of *Lm*TRYP6 protein

Once the final model was built up, the possible binding sites of *Lm*TRYP6 were searched and structural comparison of the template and the models were built. In this study, active sites were searched to identify protein active sites and binding sites by locating cavities in the *Lm*TRYP6 structure. The largest site was automatically displayed on the structure which is conserved in all peroxiredoxin sequences; hence, their biological function may be identical. In fact, from the structure–structure comparison of template, and form final refined models it was found that the peroxidatic active site is located in a pocket formed by the residues Pro45, Met46, Thr49, Val51, Cys52, Arg128, Met147 and Pro 148 (Fig. 5). The catalytic Cys52

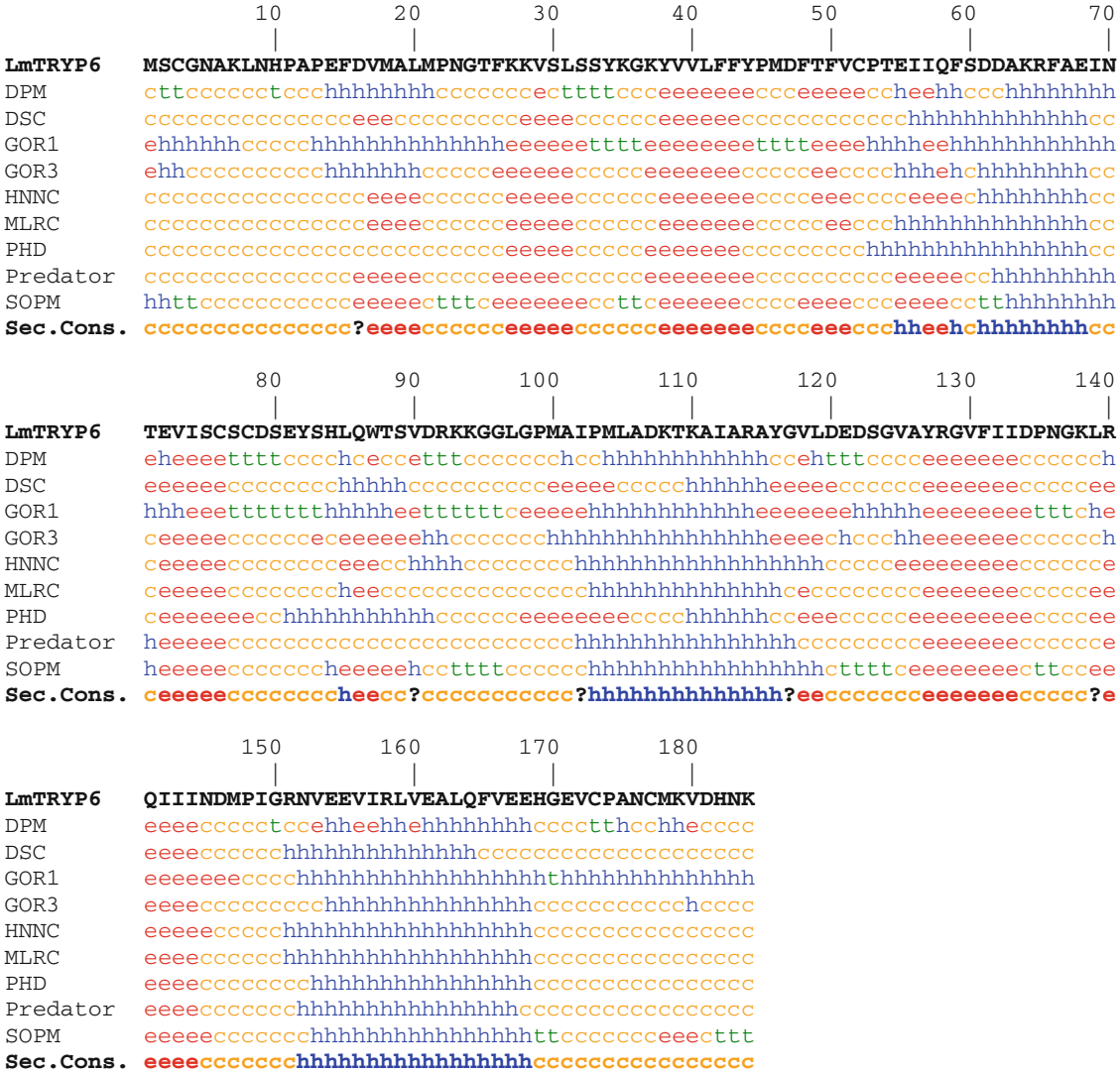

Fig. 3 Prediction of the secondary structure of *Lm*TRYP6 by the server (http://npsapbil.ibcp.fr/cgibin/npsa_automat.pl?page=/NPSA/npsa_seccons.html) using different methods. *c* coil, *h* helix, *e* strand, *t* turn

(Cp-residue), located in the first turn of helix αB, is in van der Waals with a Pro45, a Thr49 and an Arg128 that are absolutely conserved in all known Prx sequences.

Molecular dynamics simulations

Molecular dynamics simulations were carried out (1 ns) for the minimized *Lm*TRYP6 model and the *Cf*TRYP crystal structure (PDB code = 1e2y). The RMSD and RMSF values for the backbone atoms were used to understand the response behavior (Fig. 6). After equilibration, the RMSD to the initial structure were in the range from 0.7 to 1.7 and 0.9 to 5.4 Å for the *Lm*TRYP6 model and the *Cf*TRYP, respectively. Along the simulation, the radius of gyration of the *Lm*TRYP6 model and the *Cf*TRYP, range from 16.87 to 16.46 and 17.11 to 15.71 Å, respectively (data not shown). These results are implying a more compact structure of the *Cf*TRYP than *Lm*TRYP6, after the simulation. The 2D-RMSD plot, where the RMSD of every conformation to all other conformations of a simulation is shown, demonstrated that the conformational space sampled by *Cf*TRYP in the simulations was larger than *Lm*TRYP6 model (Fig. 6a). Average RMSF values in the MD simulation were usually considered as the criterion for overall flexibility of the system. RMSFs of backbone atoms against each residue where calculated over the last 900 ps for both enzymes. As shown in Fig. 6b, RMSFs in most regions of *Lm*TRYP6 merely showed slight fluctuation than *Cf*TRYP, indicating that the *Lm*TRYP6 are relatively more stable than *Cf*TRYP. On the contrary of *Lm*TRYP6, the N- and C-terminal region of the *Cf*TRYP exhibited steep RMSF-fluctuations indicting that these region are more flexible. Given the decrease of the flexibility of the Cr residue (Cys173) belonging from C-terminal of the

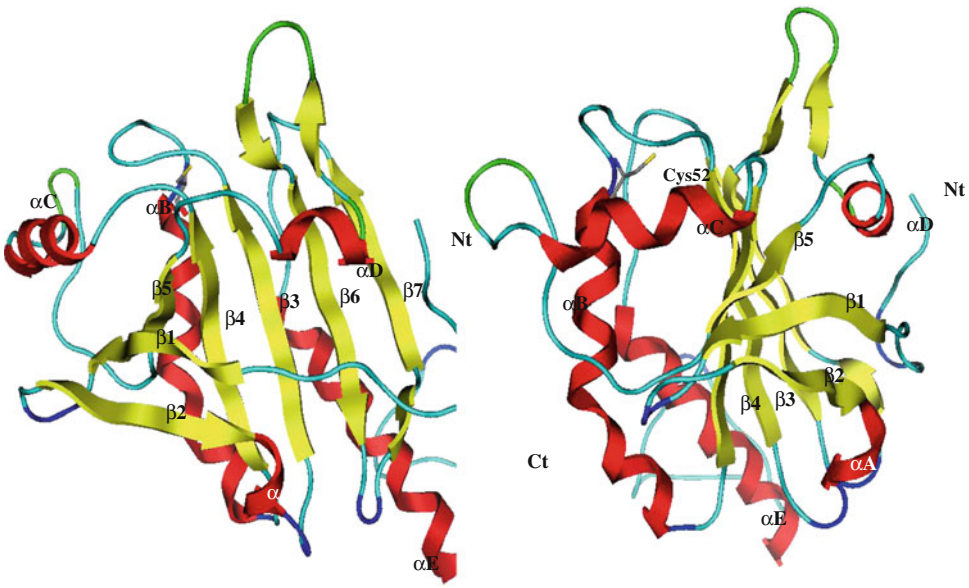

Fig. 4 Cartoon representation of the three dimensional structure of *Lm*TRYP6 model

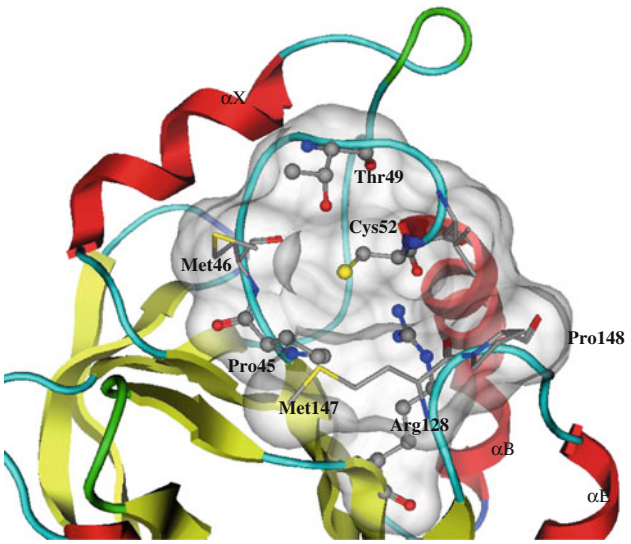

Fig. 5 Surface GRASP representation of the catalytic pocket of the peroxidatic. Amino acids involved in the pocket (Pro45, Met46, Thr49, Val51, Cys52, Arg128, Met147 and Pro 148) were represented by *sticks* and indicated

*Lm*TRYP6, it is tempting to speculate that the resolving activity of Cr is less than in *Cf*TRYP at 310 K but may be increase at hight temperature.

The decamers was formed via the associations involving only two distinct interfaces, types A and B (Fig. 7a).

Discussion

Genome sequencing in many organisms and subsequent abundant data in genbank lead us to find ortholog and paralog genes and subsequently compare biomolecules, analyze biochemical protein functions, characterize the types of protein structures such as first, secondary and tertiary structure, and predict their topology and so on using the full advancement of the bioinformatics analysis data before applying and designing of the experimental biological analysis in laboratories.

Recently, many peroxiredoxins were characterized in different organisms like *Schizosaccharomyces pombe* [32], black tiger shrimp (*Penaeus monodon*) [33], *Arabidopsis thaliana* [34], *Zhikong scallop Chlamys farreri* [35], *Xenopus embryos* [36], *Leishmania* spp. [8, 11, 16, 18] and etc.

As shown in Genbank, *L. major* has seven members of tryparedoxin peroxidase family. In this study, TRYP6 from *L. major* (MRHO/IR/75/ER) was characterized. The result of this analysis is an essential step to understand the detoxification basis of antioxidant process in *L. major* (MRHO/IR/75/ER) which subsequently could introduce a critical antigen for designing of drugs to fight the parasites.

The sequence of *Lm*TRYP6 protein was predicted virtually, which is, contained 184 amino acids with molecular weight of 20,547.56 Daltons (about 20 kDa) and isoelecterical point of 6.1101. As shown in Fig. 3, predicted secondary structure of *Lm*TRYP6 protein showed that it contains seven β-strands, five α-helices and remaining coil structures. Sequence analysis also revealed that *Lm*TRYP6 belongs to peroxiredoxin family. As illustrated based on sequence alignment of peroxiredoxins from all biological kingdoms in agreement with Hofmann et al. [37], five major clusters have been distinguished among peroxiredoxins including Prx1, Prx6, Prx5, Tpx and BCP subfamilies [37, 38]. Typical 2-Cys peroxiredoxins have conserved features across all kingdoms with at least 30% or higher

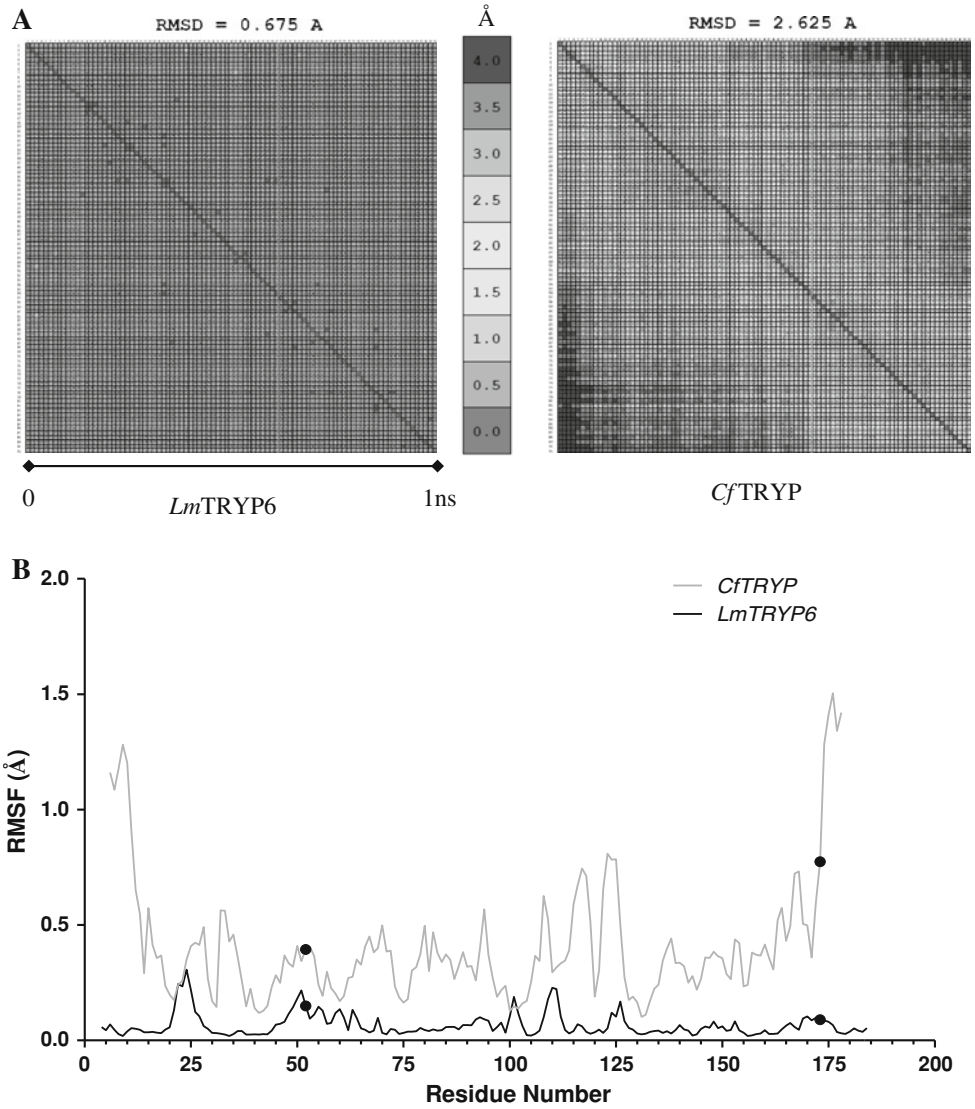

Fig. 6 Molecular dynamics simulation: **a** 2D-RMSD in simulation of *Lm*TRYP6 (*left panel*) and *Cf*TRYP (*right panel*). The root mean square deviation of every conformation to all other conformations of simulation, as a function of time of back-bone atoms during a 1 ns simulation, is shown in the 2D-RMSD (*dark color* indicated hight deviation). **b** Global fluctuations (RMSF) of *Lm*TRYP6 and *Cf*TRYP during the last 900 ps of simulation at 310 K. Cp (Cys52) and Cr (Cys173) were indicated by a *black circle*

sequence identity. In terms of labels based on mechanism, all typical 2-Cys peroxiredoxins is categorized under Prx1 or Prx6 subfamilies. Therefore, *Lm*TRYP6 seems to be belonging to either Prx1 or Prx6. Members of Prx6 subfamily studied thus far have a C-terminal extension that is even longer than the Prx1 enzymes. These enzymes (Prx6) are 111 distinct in that the two Cys residues, resolving and peroxidatic, are positioned 35 residues away from each other and is often present in close association with a third Cys in a CXDWWFC(R) motif. The third Cys is not essential but may facilitate catalysis under certain circumstances [39]. PrxI subfamily includes four of the six mammalian peroxiredoxins. These isoforms have the conserved N- and C-terminal Cys residues that are separated by 121 residues [40, 41]. The characteristic feature of this category is the presence of two highly conserved redox active-Cysteine residues: the peroxidatic Cysteine (Cys52) and the resolving Cysteine (Cys173) present in the Val-Cys-Pro catalytic domains. Multiple alignment protein showed that *Lm*TRYP6 possess two conserved Cys52 and Cys173 that are separated by 121 amino acid residues like Prx1.

The presence of the C-terminal peptide, Gln185 to Gln197 is essential for membrane binding, as the *Lm*TRYP6 did not possess this domain, therefore it should be a Cytosolic and soluble form of the enzyme.

Characterization of the gene and identification of functional specificity and biological function of the protein which is linked to its 3D folding structure are required to design appropriate experiments for further studies including site-directed mutant agenesis in order to confirm the hypothetical functions attributed to the protein domains and individual amino acids, identifying active sites, improving inhibitors for a given binding site, modeling substrate specificity, identifying and predicting antigenic epitopes, inferring function from calculated electrostatic potential surrounding the protein, and docking of simulation protein–protein. Accessing 3D folding structure would

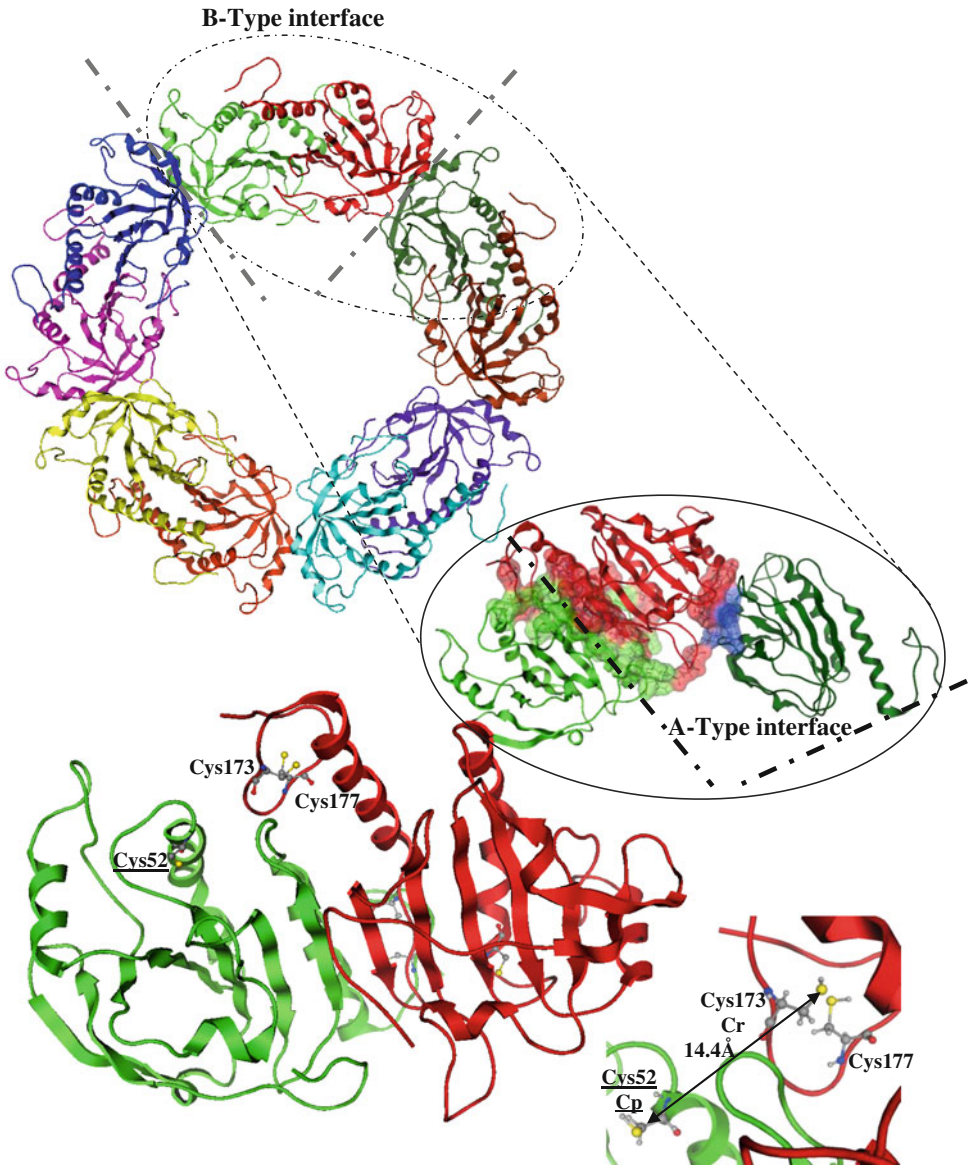

Fig. 7 Quaternary structures of LmTRYP6. **a** Model structure of a decamer of the LmTRYP6 with A-type dimer and B-type dimer association, surface contact is shown as surface GRASP representation. **b** B-type dimer of the LmTRYP6. Cp (Cys52) (*underlined*) and Cr (Cys173) were represented by *stick* and indicated

be done with the relatively slow and expensive experimental methods supplemented by theoretical methods. Bioinformatics is a theoretical method, which provides computational tools such as homology modeling for predicting, analyzing and visualizing of protein 3D structures.

Amino acid sequence analysis of *Lm*TRYP6 revealed that they are closely related to the crystal structure of *Cf*TryP from *C. fasciculata.* To define the structural and functional characteristics, the 3D structure of *Lm*TRYP6 was built by homology modeling and simulations. The protonation states of the *Lm*TRYP6 using a method based on PROPKA showed that the Cys52 has 0.85 pKa value [42]. This low pKa value may be correlated to the high reactivity of the Cp-residue as it has been reported in peroxiredoxins [39]. According to the homology sequence, the *Lm*TRYP6 share Cys177 in the place of Trp among the Prx1 group. These two Cys, Cys173 (pKa = 9.51) and Cys177 (pKa = 7.56), were about 32 Å away from the peroxidatic Cys52 (Cp), ruling out any direct involvement in the direct (auto) resolving for the same monomer and further strengthened the importance of the dimerization for the resolving step. Thus, the dimers and the decamers were built using the same template (PDB code = 1e2y) and the generated models were then subjected to molecular mechanics optimization (Fig. 7).

The *Lm*TRYP6 protein has α/β hydrolase fold similar to that present in all peroxiredoxins (Fig. 4). A core structure-sheet and five α helices which are organized as a central 7-stranded $\beta 2$-$\beta 1$-$\beta 5$-$\beta 4$-$\beta 3$-$\beta 6$-$\beta 7$ (strand $\beta 1$ and $\beta 6$ are anti-parallel) surrounded by 2-stranded β-hairpin, α helices A and D on one side, and α helices B, C and E on the other side.

The peroxidatic active site is located in a pocket formed by the residue Pro45, Met46, Thr49, Val51, Cys52,

Table 2 The B-type interface was stabilized by 12 hydrogen bonds, 12 hydrophobics and 4 ions interaction and A-type interface was stabilized only by four hydrogen bonds

B-type interface											
Hydrogen bonds				Hydrophobic interaction				Ion interaction			
Ch	Res. atom	Ch	Res. atom	Ch	Res. atom	Ch	Res. atom	Ch	Res. atom	Ch	Res. atom
1	K7.NZ	2	D122.OD1	1	L8.CD2	2	I144.CD1	1	K7.NZ	2	D122.OD1
1	N9.ND2	2	D122.OD2	1	V51.CG2	2	V172.CG1	1	D122.OD1	2	LYS7.NZ
1	T54.OG1	2	A175.N	1	I142.CB	2	I144.CG2	1	R140.NH2	2	D146.OD2
1	D122.OD1	2	K7.NZ	1	I143.CB	2	I143.CD1	1	D146.OD2	2	R140.NH2
1	D122.OD2	2	N9.ND2	1	I143.CD1	2	L159.CD1				
1	R140.NH2	2	D146.OD2	1	I144.CD1	2	L8.CD1				
1	Q141.NE2	2	N145.OD1	1	I144.CG2	2	I142.CB				
1	N145.OD1	2	Q141.NE2	1	I149.CG1	2	L159.CD2				
1	D146.OD2	2	R140.NH2	1	L159.CD1	2	I143.CD1				
1	V153.N	2	N176.ND2	1	L159.CD2	2	I149.CG1				
1	A175.N	2	T54.OG1	1	L163.CD2	2	I149.CG2				
1	N176.ND2	2	V153.N	1	V172.CG1	2	V51.CG2				

A-type interface			
Hydrogen bonds			
Chain	Res. atom	Chain	Res. atom
1	ASP79.OD1	10	SER80.N
1	SER80.N	10	ASP79.OD1
1	LYS108.O	10	LYS110.NZ
1	LYS110.NZ	10	LYS108.O

Arg128, Met147 and Pro 148 (Fig. 5). The catalytic Cys52 (Cp-residue), located in the first turn of helix αB, is in van der Waals with a Pro45, a Thr49 and an Arg128 that are absolutely conserved in all known Prx sequences.

The decamers was formed via the associations involving only two distinct interfaces. The B-type interface involves the edge-to-edge association of stands β7 of the central β-sheet of two *Lm*TRYP6 chains to make an extended 14-stranded β-sheet (Fig. 7b). However, the A-type interface is a tip-to-tip association centered on the helix αC packing against its counterpart in the other chain. The B-type interface was stabilized by 12 hydrogen bonds, 12 hydrophobics and 4 ions interaction. In contrast, A-type interface was stabilized only by 4 hydrogen bonds (Table 2). These few stabilized interactions in the A-type interface showed that the decamers was none physiologically relevant state as it was reported by Karplus and Hall [39]. The Cr residue (Cys173) from one monomer is about 14.4 Å away from Cp (Fig. 7b).

Cutaneous leishmaniasis (CL) due to *L. major* is prevalent in many countries worldwide including many rural areas in 15 of 30 provinces in Iran. Also, recent reports indicated an outbreak of the disease [43]. Antimoniate is a current choice for CL but there are expanding evidences of developing clinical resistance toward this line of drugs. It is hypothesized that the resistance is related to tryparedoxin peroxidase over expression in parasite [44–46].

Thus, the study of defensive mechanisms in the medically important protozoa parasite, *L. major*, has attracted considerable attention because of the awareness that toxic peroxides generated by oxidative stress are eliminated through a unique system of enzyme cascade including tryparedoxin peroxidase as an important stuff for survival during oxidative stress, enhancing the infectivity and survival abilities and altering its capability to drug response. Therefore, in view of the above rational, tryparedoxin peroxidase could be considered as an important target for developing anti-leishmanial drugs to fight an important human pathogen.

In the context of molecular dynamics, questions regarding the relationship among enzyme activity, solvent effects, protein stability, and flexibility often arise.

References

1. Channon JY, Roberts MB, Blackwell JM (1984) A study of the differential respiratory burst activity elicited by promastigotes and amastigotes of *Leishmania donovani* in murine resident peritoneal macrophages. Immunology 53:345–355

2. Murray HW (1982) Cell-mediated immune response in experimental visceral leishmaniasis II. Oxygen-dependent killing of intracellular *Leishmania donovani* amastigotes. J Immunol 129:351–357
3. Muller S, Liebau E, Walter RD, Krauth-Siegel RL (2003) Thiol based redox metabolism of protozoan parasites. Trends Parasitol 19:320–328
4. Tovar J, Cunningham ML, Smith AC, Croft SL, Fairlamb AH (1998) Down-regulation of *Leishmania donovani* trypanothione reductase by heterologous expression of a trans-dominant mutant homologue: effect on parasite intracellular survival. Proc Natl Acad Sci USA 95:5311–5316
5. Krauth-Siegel RL, Meiering SK, Schmidt H (2003) The parasite-specific trypanothione metabolism of *trypanosoma* and *Leishmania*. Biol Chem 384:539–549
6. Dumas C, Ouellette M, Tovar J, Cunningham ML, Fairlamb AH, Tamar S, Olivier M, Papadopoulou B (1997) Disruption of the trypanothione reductase gene of *Leishmania* decreases its ability to survive oxidative stress in macrophages. EMBO J 16: 2590–2598
7. Schmidt A, Krauth-Siegel RL (2002) Enzymes of the trypanothione metabolism as targets for antitrypanosomal drug development. Curr Top Med Chem 2:1239–1259
8. Levick MP, Tetaud E, Fairlamb AH, Blackwell JM (1998) Identification and characterisation of a functional peroxidoxin from *Leishmania major*. Mol Biochem Parasitol 96:125–137
9. Zarley JH, Britigan BE, Wilson ME (1991) Hydrogen peroxide-mediated toxicity for *Leishmania donovani chagasi* promastigotes. Role of hydroxyl radical and protection by heat shock. J Clin Invest 88:1511–1521
10. Wilson ME, Andersen KA, Britigan BE (1994) Response of *Leishmania chagasi* promastigotes to oxidant stress. Infect Immun 62:5133–5141
11. Lin YC, Hsu JY, Chiang SC, Lee ST (2005) Distinct overexpression of cytosolic and mitochondrial tryparedoxin peroxidases results in preferential detoxification of different oxidants in arsenite-resistant *Leishmania amazonensis* with and without DNA amplification. Mol Biochem Parasitol 142:66–75
12. Walker J, Acestor N, Gongora R, Quadroni M, Segura I, Fasel N, Saravia NG (2006) Comparative protein profiling identifies elongation factor-1beta and tryparedoxin peroxidase as factors associated with metastasis in *Leishmania guyanensis*. Mol Biochem Parasitol 145:254–264
13. Harder S, Bente M, Isermann K, Bruchhaus I (2006) Expression of a mitochondrial peroxiredoxin prevents programmed cell death in *Leishmania donovani*. Eukaryot Cell 5(5):861–870
14. Chen L, Xie QW, Nathan C (1998) Alkyl hydroperoxide reductase subunit C (AhpC) protects bacterial and human cells against reactive nitrogen intermediates. Mol Cell 1(6):795–805
15. Bryk R, Griffin P, Nathan C (2000) Peroxynitrite reductase activity of bacterial peroxiredoxins. Nature 407(6801):211–215
16. Castro H, Budde H, Flohé L, Hofmann B, Lünsdorf H, Wissing J, Tomás AM (2002) Specificity and kinetics of a mitochondrial peroxiredoxin of *Leishmania infantum*. Free Radic Biol Med 33(11):1563–1574
17. Castro H, Sousa C, Santos M, Cordeiro-da-Silva A, Flohé L, Tomás AM (2002) Complementary antioxidant defense by cytoplasmic and mitochondrial peroxiredoxins in *Leishmania infantum*. Free Radic Biol Med 33(11):1552–1562
18. Flohé L, Budde H, Bruns K, Castro H, Clos J, Hofmann B, Kansal-Kalavar S, Krumme D, Menge U, Plank-Schumacher K, Sztajer H, Wissing J, Wylegalla C, Hecht HJ (2002) Tryparedoxin peroxidase of *Leishmania donovani*: molecular cloning, heterologous expression, specificity, and catalytic mechanism. Arch Biochem Biophys 397(2):324–335
19. Barr SD, Gedamu L (2001) Cloning and characterization of three differentially expressed peroxidoxin genes from *Leishmania chagasi*. Evidence for an enzymatic detoxification of hydroxyl radicals. J Biol Chem 276(36):34279–34287
20. Khalil EAG, El Hassan Zijlstra EE, Mukhtat MM, Ghalib HW, Musa B, Ibrahim ME, Kamil A, Elsheikh M, Modabber F (2000) Autoclaved *L. major* vaccine for prevention of visceral leishmaniasis: a randomised, double-blind, BCG-controlled trial in Sudan. Lancet 356:1565–1569
21. Nadim A, Javadian E (1998) Leishmanization in Iran. In: Walton B, Wijeyaretne PM, Modabber F (eds) Research on strategies for the control of Leishmaniasis. International Development Research Center, Ottawa, pp 336–369
22. Sharifi I, FeKri AR, Aflatonian MR, Khamesipour A, Nadim A, Mousavi MR, Momeni AZ, Dowlati Y, Godal T, Zicker F, Smith PG, Modabber F (1998) Randomised vaccine trial of single dose of killed *Leishmania major* plus BCG against anthroponotic cutaneous leishmaniasis in Bam, Iran. Lancet 351(9115): 1540–1543
23. Momeni AZ, Jalayer T, Emamjomeh M, Khamesipour A, Zicker F, Ghassemi RL, Dowlati Y, Sharifi I, Aminjavaheri M, Shafiei A, Alimohammadian MH, Hashemi-Fesharki R, Nasseri K, Godal T, Smith PG, Modabber F (1997) A randomised, double-blind, controlled trial of a killed *L. major* vaccine plus BCG against zoonotic cutaneous leishmaniasis in Iran. Vaccine 17(5):466–472
24. Bahar K, Dowlati Y, Shidani B, Alimohammadian MH, Khamesipour A, Ehsasi S, Hashemi-Fesharki R, Ale-Agha S, Modabber F (1996) Comparative safety and immunogenicity trial of two killed *Leishmania major* with or without BCG in human volunteers. Clin Dermatol 14(5):489–495
25. Khamesipour A, Dowlati Y, Asilian A, Hashemi-Fesharki R, Javadi A, Noazin S, Modabber F (2005) Leishmanization: use of an old method for evaluation of candidate vaccines against leishmaniasis. Vaccine 23(28):3642–3648
26. Hendricks LD, Wood DE, Hajduk ME (1978) Haemoflagellates commercially available liquid media for rapid cultivation. Parasitology 76:309–316
27. Ozbilgin A, Tas S, Atambay M, Alkan Z, Ö zbel Y (1995) Comparison of liquid and biphasic media in in vitro cultivation of *Leishmania infantum* promastigotes. Acta Parasitol Turc 19:1–5
28. Castro H, Sousa C, Novais M, Santos M, Budde H, Cordeiro-da-Silva A, Flohe L, Tomas AM (2004) Two linked genes of *Leishmania infantum* encode tryparedoxins localised to cytosol and Mitochondrion. Mol Biochem Parasitol 136:137–147
29. Eisenberger CL, Jaffe CL (1999) *Leishmania*: identification of old world species using a permissively primed intergenic polymorphic-polymerase chain reaction. Exp Parasitol 91:70–77
30. Altschul SF, Madden TL, Schaffer AA, Zhang J, Zhang Z, Miller W, Lipman DJ (1997) Gapped BLAST and PSI-BLAST: a new generation of protein database search programs. Nucleic Acids Res 25:3389–3402
31. Altschul SF, Wootton JC, Gertz EM, Agarwala R, Morgulis A, Schaffer AA, Yu Y (2005) Protein database searches using compositionally adjusted substitution matrices. FEBS J 272: 5101–5109
32. Kang GY, Park EH, Lim CJ (2008) Molecular cloning, characterization and regulation of a peroxiredoxin gene from *Schizosaccharomyces pombe*. Mol Biol Rep 35(3):387–395
33. Qiu L, Ma Z, Jiang S, Wang W, Zhou F, Huang J, Li J, Yang Q (2010) Molecular cloning and mRNA expression of peroxiredoxin gene in black tiger shrimp (*Penaeus monodon*). Mol Biol Rep 37(6):2821–2827
34. Finkemeier I, Goodman M, Lamkemeyer P, Kandlbinder A, Sweetlove LJ, Dietz KJ (2005) The mitochondrial type II peroxiredoxin F is essential for redox homeostasis and root growth

of *Arabidopsis thaliana* under stress. J Biol Chem 280(13): 12168–12180
35. Cong M, Ni D, Song L, Wang L, Zhao J, Qiu L, Li L (2009) Molecular cloning, characterization and mRNA expression of peroxiredoxin in *Zhikong scallop Chlamys farreri*. Mol Biol Rep 36(6):1451–1459
36. Peng Y, Yang PH, Guo Y, Ng SS, Liu J, Fung PC, Tay D, Ge J, He ML, Kung HF, Lin MC (2004) Catalase and peroxiredoxin 5 protect *Xenopus embryos* against alcohol-induced ocular anomalies. Invest Ophthalmol Vis Sci 45(1):23–29
37. Hofmann B, Hecht HJ, Flohé L (2002) Peroxiredoxins. Biol Chem 383:347–364
38. Trivelli X, Krimm I, Ebel C, Verdoucq L, Prouzet-Mauléon V, Chartier Y, Tsan P, Lauquin G, Meyer Y, Lancelin JM (2003) Characterization of the yeast peroxiredoxin Ahp1 in its reduced active and over oxidized inactive forms using NMR. Biochemistry 42:14139–14149
39. Flohe L, Harris JR (2007) Peroxiredoxin systems, subcellular biochemistry. Springer, Germany
40. Seo MS, Kang SW, Kim K, Baines IC, Lee TH, Rhee SG (2000) Identification of a new type of mammalian peroxiredoxin that forms an intramolecular disulfide as a reaction intermediate. J Biol Chem 275:20346–20354
41. Rhee SG, Chae HZ, Kim K (2005) Peroxiredoxins: a historical overview and speculative preview of novel mechanisms and emerging concepts in cell signaling. Free Radic Biol Med 38:1543–1552
42. Li H, Robertson AD, Jensen JH (2005) Very fast empirical prediction and rationalization of protein pK_a values. Proteins 61:704–721
43. IMHME (2009) Official report of *Leishmania* cases in Iran. Iran Ministry of Health & Medical Education (IMHME)
44. Mittal K, Rai S, Ravinder A, Gupta S, Sundar S, Goyal N (2007) Characterization of natural antimony resistance in *Leishmania donovani* isolates. Am J Trop Med Hyg 76:681–688